SUPERSONIC INLET DUCT UNSTART INDUCED BY FUEL JET INJECTION

Hyungrok Do
Mechanical Engineering Department, Stanford University, Stanford CA 94305
hyungrok@stanford.edu

Seong-kyun Im
Mechanical Engineering Department, Stanford University, Stanford CA 94305
sim3@stanford.edu

M. Godfrey Mungal
Mechanical Engineering Department, Stanford University, Stanford CA 94305
School of Engineering, Santa Clara University, Santa Clara CA 95053
mungal@stanford.edu, mgmungal@scu.edu

Mark A. Cappelli
Mechanical Engineering Department, Stanford University, Stanford CA 94305
cap@stanford.edu

ABSTRACT

A high pressure transverse air jet is injected into a Mach 5 supersonic model inlet to induce inlet unstart. Planar laser Rayleigh scattering from condensed CO_2 particles is used to visualize flow dynamics during the unstart process, while in some cases, wall pressure traces are simultaneously recorded. Boundary layer separation triggered by downstream surface pressure rise is found to precede the formation of a shock system, instantly followed by inlet unstart. Studies conducted over a range of initial inlet flow conditions reveal that the presence of turbulent wall boundary layers affects the unstart dynamics. It is found that relatively thick turbulent boundary layers facilitate faster inlet unstart, when compared to thin, laminar boundary layers.

INTRODUCTION

Inlet unstart has been described as the disgorgement of a shock system at the inlet throat of a scramjet/ramjet engine (Emami et al. 1995). If not avoided, it can cause in-flight engine malfunctioning (Wieting 1976; Hawkins and Marquart 1995; Rodi et al. 1996; Shimura et al. 1998; O'Byrne et al. 2000; Wagner et al. 2008, 2009a, 2009b). Most frequently occurring during the transition to scramjet mode in the flight Mach number ranges of 3 to 6 (Andreadis, 2004), unstart is believed to be caused by the thermal choking (Mashio et al. 2001) of the internal supersonic flow triggered by increased heat release in the combustor (Heiser and Pratt 1993; Sato et al. 1997; Kodera et al. 2003). The heat release in the combustor is followed by a pressure rise in the inlet duct and boundary layer separation/growth, reducing the supersonic core flow area, and forcing the internal flow into a subsonic regime (McDaniel and Edwards 2001). Recently, in a ground test facility that mimics the thermal choking by the downstream movement of a mechanical flap, Wagner et al. (2008, 2009a, 2009b) confirmed the presence of the separated boundary layer using Particle Image Velocimetry (PIV), and captured (via high speed Schlieren photography) the formation and dynamics of an unstart shock system that interacted with the boundary layers.

Past studies have examined methods such as the introduction of isolators (Curran et al. 1996; Sato et al. 1997; Wang and Le 2000; Tam et al. 2008), boundary layer bleeding (Kodera et al. 2003) and vortex generator jets (Valdivia et al. 2009), as a means of avoiding or delaying inlet unstart. The latter two methods seek to influence the evolution of the boundary layer during the upstream propagation of flow disturbances that originate from the combustor. Recording and understanding the dynamics of boundary layer evolution during unstart is critical to the development of such unstart mitigation strategies. Studies will therefore require diagnostic methods that are capable of resolving the structure of boundary layers, and shock-boundary layer interactions.

This paper describes a study of the unstart phenomenon in a supersonic inlet, triggered by mass injection downstream of the inlet. The jet/supersonic flow and ensuing dynamics is highly three-dimensional, and we visualize the unstart flow features (e.g. boundary layers, shock-boundary layer interactions) using Planar Laser Rayleigh Scattering (PLRS) from condensed CO_2 particles (Miles and Lempert (1997); Wu et al. (2000); and Poggie et al. (2004)). The use of this PLRS visualization technique allows us to investigate the evolution of fine scale flow structures under unstart flow conditions produced in a model inlet built into a supersonic wind tunnel. The current study reveals that the flow features emerging during unstart are influenced by wall boundary layer conditions, which, in some cases, can either delay or accelerate the inlet unstart process.

EXPERIMENTAL SETUP

The experimental facility consists of a nominally Ma = 5 indraft wind tunnel, an integrated laser system and a jet injection module.
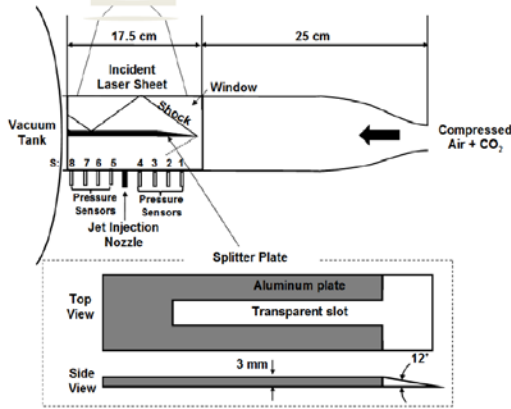

Figure 1. Experimental setup: Mach 5 wind tunnel, pressure sensors, PLRS imaging system and a splitter plate.

A schematic of the Ma = 5 wind tunnel is shown in Fig. 1. High pressure air (p_0 = 350 kPa and T_0 = 300 K) containing CO_2 (approximately 25 % by volume) expands through a converging/diverging nozzle (25:1 area ratio) to establish a relatively uniform Ma = 5 flow in a rectangular test section (4 cm × 4 cm cross-sectional area). The exit of the tunnel is connected to a vacuum tank that accommodates the incoming mass flow for approximately 5 seconds of run time. The static pressure, temperature and velocity of the flow in the test section are approximately 1 kPa, 50 K and 720 m/s, respectively.

Windows on both sides of the test section and transparent upper/lower walls allow optical access. Splitter plates (aluminum plate) of 3 mm thickness and 4 cm width, having a sharp leading wedge and a transparent slot of an embedded acrylic plate, are installed in the test section to define various model inlet geometries (Fig. 2). For example, the sharp leading wedge of an asymmetric design (12° angled wedge in the top half of channel), as shown in Fig. 1, is used to generate a relatively shock-free flow in the lower half (Case II in Fig. 2 (b)). In this configuration (Case II), the jet (ID = 3 mm) is injected through a relatively thick boundary layer (which originated upstream near the throat of the tunnel) into the flow of the model inlet/isolator defined in the lower half of the tunnel. The boundary layer on the upper wall of this inlet (i.e. on the bottom surface of the splitter plate) grows naturally from the leading edge of the plate. Three other model inlet/isolator configurations are studied. All of the configurations are summarized in Fig. 2, which also depicts the flow regions imaged by planar Rayleigh scattering (rectangles of dashed lines).

Static pressure traces are recorded on the bottom wall of the tunnel straddling a jet injection nozzle, using eight fast response (100 kHz) pressure sensors (S1 – S8: PCB Piezotronics, Model 113A26). The sensors and the jet
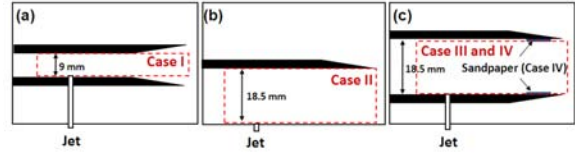

Figure 2. The region of interest in each case (Case I through Case IV) and configurations of the splitter plates.

injection nozzle, placed between S4 and S5, are separated by 15 mm along the centerline of the bottom wall parallel to the freestream flow direction: S1 and S8 are located 60 mm upstream and downstream from the nozzle, respectively. The distance between the tip of the splitter plate (270 mm downstream from the converging/diverging nozzle throat) and the jet nozzle is 75 mm.

Rayleigh scattering is carried out with a Nd:YAG laser (New Wave, Gemini PIV) capable of generating approximately 100 mJ/pulse (532 nm wavelength) with 10 Hz pulse repetition. The laser beam is transformed into a thin sheet of 0.5 mm thickness using a combination of two concave cylindrical lenses (200 mm focal length) and a convex spherical lens (250 mm focal length). The laser sheet spans a plane along the center line of the tunnel parallel to the freestream direction. Light scattered along a direction normal to the laser sheet is captured by an unintensified CCD camera (La Vision, Imager Intense, 1376 by 1040 pixel array) instrumented with a 50 mm Nikon lens. CO_2 fog (solid particles) produced in the nozzle scatters laser light and evaporates under varying environments provided by primary flow features such as shockwaves and boundary layers where the local static temperature/pressure increases. Shockwaves, boundary layers and turbulent flow structures are well illustrated in the two dimensional image illuminated by the planar laser light.

A sonic air jet is injected into the test section through a 3 mm diameter hole in the bottom wall resulting in a flow disturbance and an overall increase in flow pressure and temperature. Relevant to the jet interaction and mixing with the supersonic free stream is the square root ratio of the jet momentum flux to that of the free stream, defined by:

$$R = \sqrt{\frac{(\rho u^2)_{jet}}{(\rho u^2)_\infty}} = \sqrt{\frac{(\gamma p M^2)_{jet}}{(\gamma p M^2)_\infty}}$$

Here, ρ, u, γ, p, and M are gas density, velocity, ratio of specific heats, pressure and Mach number of the jet (subscript jet) and freestream (subscript ∞) flow, respectively. The parameter, R, characterizes the penetration depth and mixing associated with the jet injection into a cross-flow (Smith and Mungal (1998)).
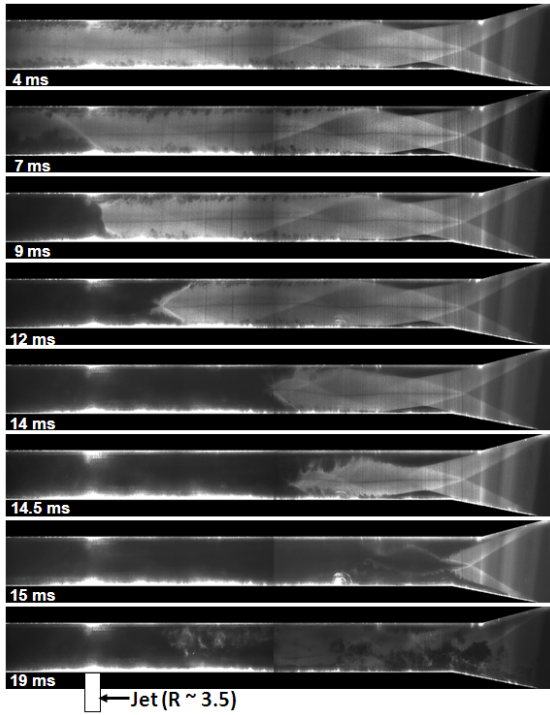
Results

Inlet Unstart in Case I

Figure 3. Time sequential PLRS images revealing flow evolution with Case I model inlet geometry.

The inlet geometry of Case I (Fig. 2 (a)) is used to simulate inlet/isolator flows in the presence of multiple shock/expansion reflections that compress and decelerate the incoming flows. Here, two identical splitter plates isolate the flow in the model inlet defined between the plates separated by 9 mm. A downstream air jet ($R = 3.5$) is injected into the inlet to induce unstart. A set of time synchronized planar laser Rayleigh scattering (PLRS) images (Fig. 3) illustrates the evolution of the flow structure while the flow unstarts. The flow structure, including shock/expansion reflections through the flow channel (Case I) before the jet is injected into the flow is visualized in the 4 ms panel of Fig. 3. At this time, 4 ms after the trigger signal activating the solenoid valve, the jet fluid has not yet arrived at the nozzle exit. At 7 ms, a jet inducing a bow shock appears and then propagates upstream of the jet nozzle followed by flow separation of both the top and bottom boundary layers (9 – 14.5 ms). These flow disturbances (e.g. shockwave, boundary layer growth/separation) reach the inlet lip, unstarting the flow, by 19 ms. At that moment, the flow near the inlet lip appears to be very unstable and the entire flow channel becomes dark due to the sublimation of the solid CO_2 particles, confirming complete inlet unstart. We see then that the downstream flow appears to unchoke by the excessive mass loading producing flow disturbances that move upstream to unstart the model inlet. We believe that the propagation of these flow disturbances may be facilitated by the presence of thicker boundary layers on the surfaces of the model inlet, and so we tested three other initial boundary layer conditions (Cases II through IV, height of the model inlets is 18.5 mm) with fixed R (4.5) to investigate the influence of the boundary layers on this unstart behavior. For the Case II geometry, our study of this process is further facilitated by pressure taps on the lower surface of the model inlet, which is also the tunnel lower wall, where a relatively thick turbulent boundary layer develops.
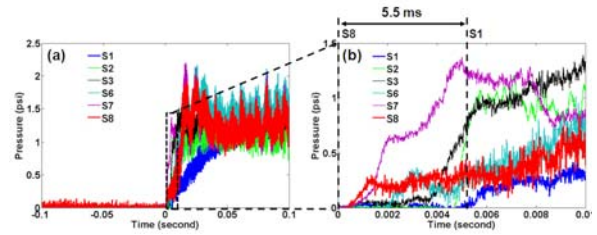
Surface Pressure Measurement in Case II

Figure 4. Pressure traces recorded on the bottom wall of the wind tunnel (Case II).

The unstart dynamics induced by air jet injection is clearly reflected in the pressure traces measured on the bottom surface of the wind tunnel (Case II). Figure 4 (a) documents the sudden pressure rise at the various locations on the lower wall (recall that the nozzle located between S4 and S5). The time reference (t = 0 sec) in this figure corresponds to the moment when the pressure first rises at the sensor located at S8. The pressure at S8 starts to rise abruptly at approximately 10 ms after the jet injection trigger signal to open the solenoid valve. Absolute pressure offsets are subtracted from the traces to illustrate relative differences between the pressure recorded before and after the jet injection. The pressure traces recorded at the locations nearest to the jet nozzle (S4 and S5, not shown) fluctuate significantly, due to flow instabilities in the near field of the jet. It is noteworthy that the first pressure increase is recorded at S8 and this high pressure region then expands towards the upstream region of the tunnel, presumably along the subsonic boundary layer, in succession through to the location at S1 (Fig. 4 (b)). This ordering in the rise in pressure confirms that unchoking originates downstream of the jet injection point, triggering tunnel unstart, i.e., the transition to subsonic flow. We conjecture that the unchoking of the flow first appears far downstream near the model exit due to the reduced supersonic core flow area by the growth/separation of boundary layers on the tunnel surfaces and the mass addition. The propagation of this high pressure region from S8 to S1 (over 12 cm distance) takes approximately 5.5 ± 0.5 ms (see Fig. 4 (b)) indicating that this pressure wave propagates at a speed of approximately 22 ± 2 m/s (a mean of 4 measurements). For comparison the freestream speed is approximately 720 m/s.

Inlet Unstart in Case II

Here, we discuss the model inlet unstart dynamics, as depicted by the PLRS studies, induced by the injected mass for the Case II model configuration (Fig. 2). This case, for which we describe the pressure traces above, is referred to here as having an asymmetric wall boundary condition, in that it is primarily distinguished by the presence of a thick turbulent boundary layer on the inlet wall through which the jet is injected. Under the current flow condition, the model inlet is found to unstart at about 21 ms after the jet is triggered (or approximately 11 ms following the first recording of a pressure disturbance at S8).
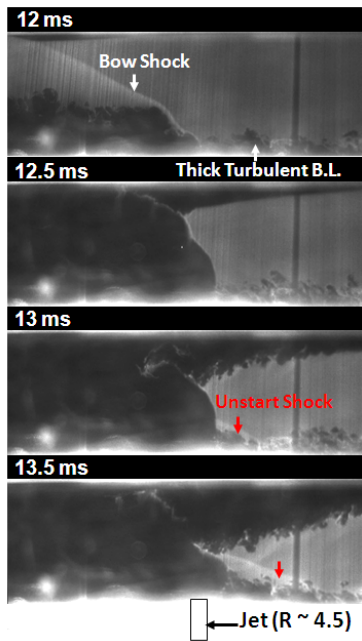

Figure 5. Time sequential PLRS images taken in the adjacent to the jet with the configurations of Case II.

The time sequential images in Figs 5 and 6 illustrate the evolution in the flow while the inlet undergoes unstart by an air jet of $R = 4.5$. The entire flow region of interest (Case II in Fig. 2 (b)) is interrogated in two separate Rayleigh scattering frames. The first frame illuminates the region in the vicinity of the jet nozzle (Fig. 5), and the other, the upstream region near the tip of the splitter plate (Fig. 6). Each imaging region covers a 5 cm width along the flow direction (from right to the left) and an 18.5 mm height. When combined, these two frames span the region within the dashed rectangular lines for Case II, in Fig. 2 (b).

The inlet unstart for this configuration is described in detail in a previous paper (Do et al. 2011) and is only briefly discussed here. Figures 5 and 6 reveal that the boundary layer growth/separation on the bottom wall of the inlet (also the bottom wall of the tunnel) propagates upstream (see frames between 13 ms (Fig. 5) and 17 ms (Fig. 6)) and generates an oblique unstart shock first appearing in front of the jet in the 13 ms panel of Fig. 5. This shock propagates upstream, and the flow unstarts shortly after the arrival of this shock at the
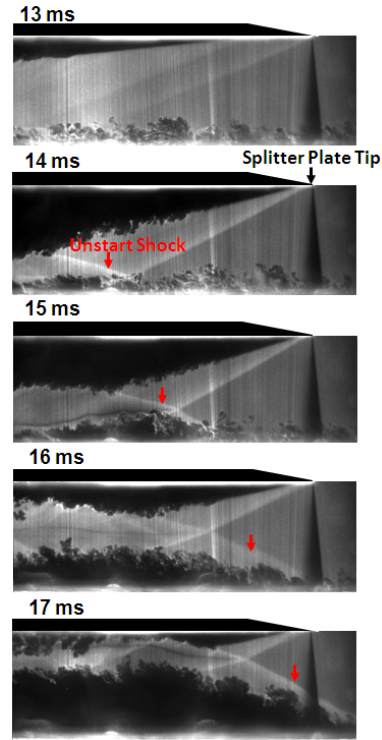

Figure 6. Time sequential PLRS images covering the first 5 cm region downstream of the splitter tip taken with the configurations of Case II.

inlet lip (Fig. 6, 17 ms). Concurrently, we also see a separated flow on the upper wall (Fig. 5, 12 ms) when the jet-induced bow shock interacts with this thin boundary layer. This upper wall disturbance also propagates upstream, preceding the unstart shock, and arrives at the tip of the splitter plate at 14 ms (Fig. 6). Trailing behind this shock is a rapidly growing boundary layer that appears to become turbulent a streamwise distance comparable to the height of the inlet channel.

Influence of boundary layers (Cases III and IV)

We find that with the Case III configuration, the oblique unstart shock that was seen to emerge in Case II does not appear and the time required for complete inlet unstart is significantly longer in comparison to the time measured for the other cases. Figure 7 presents the Rayleigh scattering images for the two frames spanning the entire region of interest, depicting the inlet flow observed for Case III over a time ranging from prior to jet injection through to flow unstart, at a time of 55 ms after jet triggering. As shown in Fig. 7 (a), (taken in the absence of the jet), the two splitter plates (with wedge outward facing) isolate the main flow from the turbulent boundary layers on the tunnel walls to define the model inlet. In this configuration, thin (initially laminar) boundary layers form on both upper and lower walls. Weak shock waves appear originating from the splitter tips, most likely due to the small but finite dimensions of the tips. The flow is seen to undergo a laminar to turbulent flow transition,
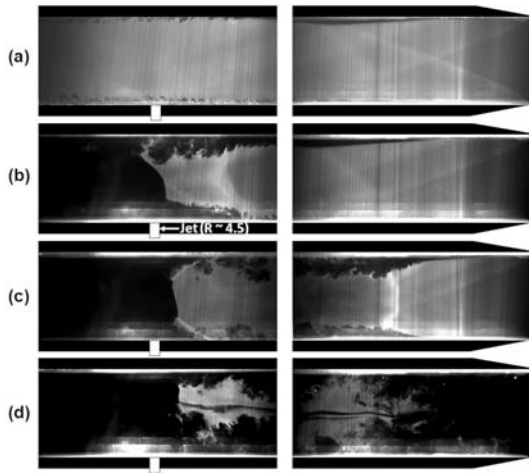
Figure 7. PLRS images with Case III configuration: (a) before the jet injection (b) the formation of a compression wave (16 – 17 ms after the jet injection), (c) a dual-shock structure (an upstream pseudo-shock and a downstream shockwave) seen in the time duration of 18 – 55 ms, and (d) breakdown of the dual-shock structure at 55 ms.

with the clear indication of relatively thin turbulent boundary layers in the downstream frame. Figure 7(b) is a similar depiction, taken shortly after jet injection (approximately 17 ms after jet triggering). At this time, we see from the brighter region that spans across the inlet at approximately 20 mm upstream of the jet, that a compression wave (presumably leading a pseudo-shock structure) forms, almost normal to the flow direction, as indicated by the diffuse, brighter signal at the center of the channel. This compression is followed by the apparent thickening of the turbulent boundary layers on both top and bottom surfaces. This compression wave propagates upstream and arrives at a position of about 27 mm from the splitter tip within about 1 ms (see Fig. 7(c)) remaining there for approximately 37 ms (from 18 ms to 55 ms). This compression wave is thicker than typical shockwaves such as the oblique unstart shock seen in Cases II, or the incident shocks originating from the splitter tips, and is not strong enough to cause transition to subsonic flow. This is evident from the fact that we still see significant Rayleigh scattering off of CO_2 fog behind this wave, as this fog would be expected to evaporate in subsonic flow regions. In addition, we see from Fig. 7(c) what appears to be a normal shock (little can be said about this with the present diagnostic) or the emergence of a lambda shock downstream of this compression wave, just upstream of the jet.

A sudden breakdown of this dual-shock structure leading to inlet flow unstart is observed (see Fig. 7(d)) at a time of 55 ms ± 0.5 ms. The breakdown occurs swiftly, within 1 ms. It is noteworthy that, in Case III, it therefore takes about 55 ms for the inlet flow to unstart – a time that is significantly longer than that of the previous two cases discussed (21 ms (Case II)). Inlet unstart appears to be delayed by the isolating of inlet flow from the thick turbulent boundary layer on the tunnel

walls. At this time, however, the physics related to the sudden breakdown of the flow structure is not resolved. We believe that this breakdown is caused by the relatively slow build-up in pressure behind the upstream pseudo-shock or pressure disturbances from the downstream region. This flow breakdown mechanism will be examined in future studies in which pressure measurements will be made along the inlet walls of the isolated flow.
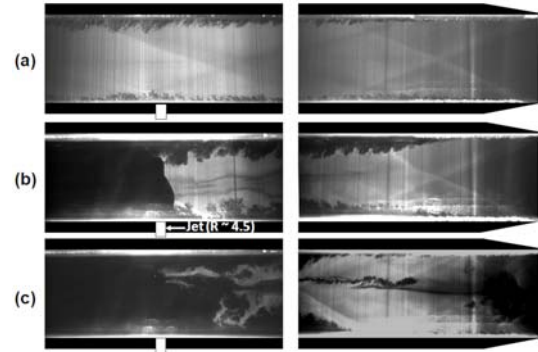

Figure 8. PLRS images with Case IV configuration: (a) before the jet injection, (b) shockwaves intersecting each other at the inlet and standing steady during 16 – 24 ms, and (c) tunnel unstart at 25 ms.

Case IV (same geometrical configuration of Case III) also isolates the inlet from this thick turbulent boundary layer, but generates its own relatively thick turbulent wall boundary layers by the use of sandpaper near the leading edge of the splitter isolator plates. Figure 8 (a) reveals the presence of turbulent boundary layers developing on the splitter plates generated by sandpaper attached 5 mm downstream of the plate tips. An earlier complete inlet unstart (25 ms) compared to that seen in Case III (55 ms), is observed with this configuration. This unstart is about as fast as that seen in Case II (21 ms), although the general flow features are more similar to those seen for Case III. A pseudo-shock structure emerges behind the intersection of the two incident shocks accompanying the development of thick turbulent boundary layers and anchoring at a quasi-stable position for 8 ms (16 ms – 24 ms after jet triggering), as seen in Fig. 8 (b). Then, a sudden break down of this flow structure (dual-shock) is observed at 25 ms (Fig. 8 (c)) instantly followed by complete inlet unstart. We attribute this early unstart, in comparison to that of Case III, to the initial turbulent boundary layers on the upper and lower inlet walls.

Summary

A Mach 5 wind tunnel was used to generate approach flow conditions for studies of unstart in model inlet/isolator flows. In the studies described, inlet unstart is generated by the injection of an air jet. Flow dynamics following jet injection were investigated with four different inlet configurations.

Planar laser Rayleigh scattering imaging was used to characterize flow features, including the evolution of boundary layers and shocks. We find that unstart flow features and the overall inlet unstart process are strongly affected by

the characteristics of the initial wall boundary layer prior to jet injection. In asymmetric inlet configurations, with a thick turbulent boundary layer on one wall, and a thin (initially laminar) boundary layer on the other (Case II), an unstart shock emerges, on the wall with an initially thick turbulent boundary layer. In Case II with the asymmetric boundary condition, complete unstart of the inlet occurs within about 21 ms. With symmetric wall configurations (i.e., cases in which wall boundary layer are similar on both sides, either turbulent or laminar), there is no oblique unstart shock. Instead, we see a relatively weak compression wave or pseudo-shock, which initially propagates upstream in advance of unstart, and remains quasi-stable for some time, until a catastrophic breakdown in the structure occurs and the inlet flow unstarts completely. The duration over which this pseudo-shock is anchored in the inlet depends on the nature of the initial boundary layer (thin laminar, or thick turbulent). With relatively thin (initially laminar) boundary layers, the pseudo-shock appears stable until 55 ms following jet injection – more than twice as long as the case in which the initial boundary layers are tripped to be turbulent (25 ms). The time for unstart in the turbulent symmetric condition is comparable to that of Case II.

REFERENCES

Andreadis D., 2004, Scramjet engines enabling the seamless integration of air & space operations. The Industrial Physicist, Aug/Sept 2004.

Curran E. T., Heiser W. H., Pratt D. T., 1996, "Fluid phenomena in scramjet combustion systems," *Annual Review of Fluid Mechanics*, Vol. 28, pp. 323–360.

Do H., Im S., Mungal M. G., Cappelli M. A., 2011, "Visualizing supersonic inlet duct unstart using planar laser Rayleigh scattering," *Experiments in Fluids*, in press, DOI 10.1007/s00348-010-1028-4.

Emami S., Trexler C. A., Auslender A. H., Weidner J. P., 1995, Experimental investigation of inlet-combustor isolators for a dual-mode scramjet at a Mach number of 4. NASA Technical Paper 3502.

Hawkins W. R., Marquart E. J., 1995, "Two-dimensional generic inlet unstart detection at Mach 2.5–5.0," *6th International Aerospace Planes and Hypersonics Technologies Conference*, Chattanooga, TN, USA.

Heiser W. H., Pratt D. T., 1993, "Hypersonic air breathing propulsion," AIAA Education Series, Washington, D.C. USA

Kodera M., Tomioka S., Kanda T., Mitani T., Kobayashi K., 2003, "Mach 6 test of a scramjet engine with boundary-layer bleeding and two-staged fuel injection," *12th AIAA International Space Planes and Hypersonic Systems and Technologies*, Norfolk, VA, USA

Mashio S., Kurashina K., Bamba T, Okimoto S., Kaji S., 2001, "Unstart phenomenon due to thermal choke in scramjet module," *AIAA/NAL-NASDA-ISAS 10th International Space Planes and Hypersonic Systems and Technologies Conference*, Kyoto, Japan

McDaniel K. S., Edwards J. R., 2001, "Three-Dimensional Simulation of Thermal Choking in a Model Scramjet Combustor," *39th Aerospace Sciences Meeting and Exhibit*, Reno, NV, USA

Miles R. B., Lempert W. R., 1997, "Quantitative flow visualization in unseeded flows," *Annual Review of Fluid Mechanics*, Vol. 29, pp. 285–326.

O'Byrne S., Doolan M., Olsen S. R., Houwing A. F. P., 2000, "Analysis of transient thermal choking processes in a model scramjet engine," *Journal of Propulsion and Power*, Vol. 16, pp. 808–814.

Poggie J., Erbland P. J., Smits A. J., Miles R. B., 2004, "Quantitative visualization of compressible turbulent shear flows using condensate-enhanced Rayleigh scattering," *Experiments in Fluids*, Vol. 37, pp. 438–454.

Rodi P. E., Emami S., Trexler C. A., 1996, "Unsteady pressure behavior in a ramjet/scramjet inlet," *Journal of Propulsion and Power*, Vol. 12, pp. 486–493.

Sato S., Izumikawa M., Tomioka S., Mitani T., 1997, "Scramjet engine test at Mach 6 flight Condition," *33rd AIAA/ASME/SAE/ASEE Joint Propulsion Conference and Exhibit*, Seattle, WA, USA.

Shimura T., Mitani T., Sakuranaka N., Izumikawa M., 1998, "Load oscillations caused by unstart of hypersonic wind tunnels and engines," *Journal of Propulsion and Power*, Vol. 14, pp. 348–353.

Smith S. H., Mungal M. G., 1998, "Mixing, structure and scaling of the jet in crossflow," *Journal of Fluid Mechanics*, Vol. 357, pp. 83 – 122.

Tam C., Eklund D., Behdadnia R., 2008, "Influence of downstream boundary conditions on scramjet-isolator simulations," *26th AIAA Applied Aerodynamics Conference*, Honolulu, HI, USA

Valdivia A., Yuceil K. B., Wagner J. L., Clemens N. T., Dolling D. S., 2009, "Active control of supersonic inlet unstart using vortex generator jets," *39th Fluid Dynamics Conference and Exhibit*, San Antonio, TX, USA

Wagner J. L., Yuceil K. B., Valdivia A., Clemens N. T., Dolling D. S., 2008, "PIV measurements of the unstart process in a supersonic inlet/isolator," *38th Fluid Dynamics Conference and Exhibit*, Seattle, WA, USA

Wagner J. L., Yuceil K. B., Clemens N. T., 2009a, "PIV Measurements of Unstart of an Inlet-Isolator Model in a Mach 5 Flow," *39th Fluid Dynamics Conference and Exhibit*, San Antonio, TX, USA.

Wagner J. L., Yuceil K. B., Valdivia A., Clemens N. T., Dolling D. S., 2009b, "Experimental investigation of unstart in an inlet/isolator model in Mach 5 flow," *AIAA Journal*, Vol. 47, pp. 1528 – 1542.

Wang X., Le J., 2000, "Computations of inlet/isolator for SCRAMjet engine," *Journal of Thermal Science*, Vol. 9, pp. 334 – 338.

Wieting A. R., 1976, "Exploratory study of transient unstart phenomena in a three-dimensional fixed-geometry scramjet engine," *NASA Technical Note, TN D-8156*.

Wu P., Lempert W. R., Miles R. B., 2000, "Megahertz Pulse-Burst Laser and Visualization of Shock-Wave/Boundary-Layer Interaction," *AIAA Journal*, Vol. 38, pp. 672 – 679.